

HELIUM EFFECTS ON VOID FORMATION IN 9Cr-1MoVNb AND
12Cr-1MoVW IRRADIATED IN HFIR*

CONF-860421--50

DE86 011766

P. J. Maziasz, R. L. Klueh, and J. M. Vitek

Metals and Ceramics Division, Oak Ridge National Laboratory,
P. O. Box X, Oak Ridge, TN 37831

Abstract

Up to 2 wt % Ni was added to 9Cr-1MoVNb and 12Cr-1MoVW ferritic steels to increase helium production by transmutation during HFIR irradiation. The various steels were irradiated to ~39 dpa. Voids were found in all the undoped and nickel-doped steels irradiated at 400°C, most of them at 500°C, but not in any of them at 300 or 600°C. Bubble formation, however, was increased at all temperatures in the nickel-doped steels. Maximum void formation was found at 400°C, but swelling remained less than 0.5% even with up to 440 appm He. Irradiation at 300 to 500°C caused dissolution of as-tempered $M_{23}C_6$ precipitates and coarsening of the lath/subgrain structure in the 9-Cr steels, whereas the microstructure generally remained stable in the 12-Cr steels. Irradiation in this temperature range also caused compositional changes in the as-tempered MC phase in all the steels, and produced combinations of fine M_6C , G, and M_2X precipitates in various steels. The subgrain boundaries appear to be strong sinks that enhance resistance to void formation. Higher helium production during irradiation appears to shorten the incubation period for void formation. The effects of helium on steady state void swelling behavior, however, remain unknown.

*Research sponsored by the Office of Fusion Energy, U.S. Department of Energy, under Contract DE-AC05-84OR21400 with the Martin Marietta Energy Systems, Inc.

By acceptance of this article, the publisher or recipient acknowledges the U.S. Government's right to retain a nonexclusive, royalty-free license in and to any copyright covering the article.

MASTER

DISCLAIMER

This report was prepared as an account of work sponsored by an agency of the United States Government. Neither the United States Government nor any agency thereof, nor any of their employees, makes any warranty, express or implied, or assumes any legal liability or responsibility for the accuracy, completeness, or usefulness of any information, apparatus, product, or process disclosed, or represents that its use would not infringe privately owned rights. Reference herein to any specific commercial product, process, or service by trade name, trademark, manufacturer, or otherwise does not necessarily constitute or imply its endorsement, recommendation, or favoring by the United States Government or any agency thereof. The views and opinions of authors expressed herein do not necessarily state or reflect those of the United States Government or any agency thereof.

1.0 Introduction

In 1971, Harkness et al. [1] observed that the void swelling resistance of bcc ferrite was better than fcc austenite in a duplex steel. Based on this and several later investigations of void formation in ferritic steels [2]–[5], various national fast breeder reactor (FBR) alloy development programs [6] began studying ferritic steels for fuel cladding in 1976. The U.S. magnetic fusion reactor (MFR) materials program included these steels as structural candidates in 1979 [7]. Void swelling resistance has been demonstrated more recently for various ferritic steels irradiated in FBRs to doses as high as 120 to 150 dpa [8]–[12]. However, helium generation in ferritic steels is very low (~ 0.1 appm He/dpa) in FBRs such as EBR-II, as seen in Fig. 1. The effect of higher helium generation on void swelling resistance is therefore a major question when considering ferritic steels for use in an MFR environment [13]–[15], where helium generation rates will be 8 to 13 appm He/dpa.

Recent work by Vitek and Klueh [16],[17] and by Gelles [18] has demonstrated that, when helium generation was increased, void formation also increased in 9- and 12-Cr ferritic steels at 400°C after ~ 39 dpa. The higher helium generation was obtained by irradiating 9Cr-1MoVNb and 12Cr-1MoVW steels in HFIR instead of EBR-II (Fig. 1). HFIR has more thermal neutrons that produce helium from a two-step transmutation reaction with nickel. Neutron irradiation studies of austenitic stainless steels have demonstrated that large amounts of helium can either increase or decrease void formation [19],[20]. Horton and Bentley [21] have shown that helium co-injected during heavy-ion irradiation of high-purity Fe-10Cr increased both the concentration of cavities and the size distribution

spreads into a bimodal indicative of subcritical cavities converting into bias-driven cavities or voids. Moreover, single and dual-beam heavy-ion irradiation studies in 12Cr-1MoVW by Ayrault [22] have shown that the presence of helium was necessary for void formation.

The purpose of this work is to further examine the effects of increased helium generation on void formation and microstructural evolution in the 9- and 12-Cr ferritic steels during neutron irradiation. Greater helium generation during HFIR irradiation was achieved by doping the steels with up to 2 wt % Ni [23], as shown for 9Cr-1MoVNb-2Ni in Fig. 1.

2.0 Experimental

The compositions of the nickel-doped and undoped heats of 9Cr-1MoVNb and 12Cr-1MoVW steels are given in Table 1. The various normalization and tempering heat treatment conditions are listed in Table 2. The 2% Ni-doped steels were tempered longer [23] at lower temperatures than the undoped alloys because previous studies showed that nickel lowered the A_{C1} (lowest critical austenite-forming) temperature. However, the 12Cr-1MoVW-1Ni had the same tempering treatment as the undoped 12-Cr steel.

Alloys were irradiated side by side in HFIR CTR-30 in the form of standard 3-mm-diam transmission electron microscopy (TEM) disks punched from 0.254-mm-thick sheet stock. Irradiation temperatures ranged from 300 to 600°C and have been verified by analysis of temperature monitors [24]. Displacement damage (including dpa due to nickel recoils) and helium generation levels were calculated by L. R. Greenwood based on dosimetry performed for this experiment [25]. HFIR neutron fluences produced 36 to 39 dpa and helium levels of ~33 appm in 9Cr-1MoVNb, ~410 appm in 9Cr-1MoVNb-2Ni, ~87 appm in 12Cr-1MoVW, ~217 appm in 12Cr-1MoVW-1Ni, and

~440 appm in 12Cr-1MoVW-2Ni. A specimen of 9Cr-1MoVNb-2Ni irradiated in FFTF at 407°C to a fluence producing 47 dpa and ~5 appm He was included in this work to separate the effects of nickel doping from those of helium on microstructural evolution under irradiation.

TEM disks were examined on a JEM 100C TEM equipped with a special objective lens polepiece designed to lower the magnetic field at the specimen. Carbon film extraction replicas were produced from as-tempered material and from selected irradiated specimens prepared in a special, shielded, hands-on facility because of the highly radioactive HFIR specimens [20]. Precipitates were studied by means of analytical electron microscopy (AEM), using either a Philips EM400 microscope equipped with a field emission gun (FEG) for very high electron intensity at small probe sizes or a JEM 2000FX microscope with an LaB₆ filament.

3.0 Results

3.1 Cavity Microstructure

A. 9Cr-1MoVNb and 9Cr-1MoVNb-2Ni steels, HFIR and FFTF

A few fine (2-5 nm in diameter) bubbles were found at 400°C in the matrix, and at 600°C along subgrain boundaries in 9Cr-1MoVNb irradiated in HFIR to ~38 dpa and ~32 appm He. Larger matrix voids (9-18 nm in diameter) were found only at 400°C [Fig. 2(a,b)]. Bubbles are cavities smaller than their critical size whose growth is gas-driven. Conversely, voids are cavities larger than their critical size whose growth is bias-driven. Some experimental guidelines for determining whether cavities are bubbles or voids have been suggested [20]. Voids formed in patches that were several microns in size, while similar adjacent patches were void-free. Cavity

swelling was about 0.2%. No bubbles were observed at either 300 or 500°C.

By contrast, HFIR irradiation of 9Cr-1MoVNb-2Ni to ~38 dpa and ~410 appm He produced significantly more fine bubbles at 300 to 600°C relative to 9Cr-1MoVNb, and also produced voids at both 400 and 500°C [see Figs. 2(c,d) and 3]. At 400°C, void formation was spatially more uniform throughout the matrix and up to several times greater in 9Cr-1MoVNb-2Ni than in the 9Cr-1MoVNb, but void sizes were similar. Void swelling appeared to be 0.3 to 0.4% in the 9Cr-1MoVNb-2Ni. At 500°C, large (20-70 nm diam) voids in 9Cr-1MoVNb-2Ni were found only inside very coarse, irradiation-produced precipitate particles [see Fig. 2(d)] tentatively identified as χ phase. Swelling appeared to be 0.1 to 0.3% in 9Cr-1MoVNb-2Ni at 500°C, whereas no void swelling was found in 9Cr-1MoVNb.

There is an obvious difference in precipitation behavior of the nickel-doped 9-Cr steel as compared to the undoped steel after HFIR irradiation at 400°C [cf Fig. 2(a) and (c)]. It raises the question of whether or not increased helium generation alone causes increased void formation. However, irradiation of the same 9Cr-1MoVNb-2Ni alloy in FFTF at 407°C to 47 dpa and ~5 appm He produced nearly the same precipitation as found during HFIR irradiation but with no matrix bubbles or voids [cf Fig. 2(c) and Fig. 4]. This comparison suggests that the increased helium generation in HFIR is primarily responsible for the increased bubble and void formation, independent of the precipitation produced in 9Cr-1MoVNb-2Ni by irradiation at about 400°C.

B. 12Cr-1MoVW, 12Cr-1MoVW-1Ni and 12Cr1MoVW-2Ni steels, HFIR

Some fine (2-5 nm in diameter) bubbles were found in the grain boundaries of 12Cr-1MoVW irradiated in HFIR at 400 to 600°C to ~37 dpa and ~87 appm He. Larger matrix voids were found at both 400 and 500°C (10-25 nm and 20-40 nm in diameter, respectively). Void formation was spatially nonuniform at both 400 and 500°C and usually occurred in the coarsest regions of the subgrain structure (Figs. 5 and 6). Many more voids were found at 400°C than at 500°C. Void swelling was about 0.1% at 400°C and less than 0.1% at 500°C. No voids or bubbles were observed at 300°C.

As with the 9-Cr steels, abundant fine bubble formation was greater at all temperatures in the nickel-doped 12-Cr steels, but voids still formed only at 400 and 500°C. At 500°C, large voids (20-80 nm in diameter) within the coarse χ phase particles of the 12Cr-1MoVW-1Ni instead of in the matrix (the 12Cr-1MoVW-2Ni has not yet been examined). At 400°C, matrix void formation was more uniform in the nickel-doped 12-Cr steels, but swelling appeared to be similar or less than in the undoped steel (Fig. 5). The matrix void size was refined in 12Cr-1MoVW-1Ni (7-19 nm in diameter) relative to 12Cr-1MoVW, but void size and distribution in 12Cr-1MoVW-2Ni were similar to the undoped steel. The as-tempered subgrain structure of the 12Cr-1MoVW-2Ni was finer than the other 12-Cr steels and at 400°C the smallest subgrains had fewer and smaller voids than the largest subgrains. The general correlation of void formation with subgrain size for all the 12-Cr steels suggests that subgrain boundaries may be strong sinks which hinder void formation.

3.2 Subgrain Structure and Precipitate Microstructure, 9- and 12-Cr Steels

A. As tempered

The 9Cr-1MoVNb steel contained polygonized, fairly dislocation-free ferrite subgrains after normalizing and then tempering for 1 h at 760°C. Coarse $M_{23}C_6$ particles were distributed along prior austenite grain boundaries and along some of the subgrain boundaries. Finer MC particles were found along subgrain boundaries and within subgrains. AEM analysis of relative phase fractions revealed 85% $M_{23}C_6$ and 15% MC. The 9Cr-1MoVNb-2Ni showed less recovery after tempering for 5 h at 700°C, with lenticular subgrains and more dislocations. There were no differences in precipitation relative to 9Cr-1MoVNb.

The 12Cr-1MoVW steel tempered for 2.5 h at 780°C had dislocation-free subgrain structure similar to the 9Cr-1MoVNb although the subgrains were finer. Because the 12Cr-1MoVW steel had more carbon than the 9Cr-1MoVNb steel, it contained more carbide precipitation (3.5 as compared to 1.4 wt % [16],[17]), which was analyzed to be 9% $M_{23}C_6$ and 1% MC. This same tempering treatment produced a similar structure in the 12Cr-1MoVW-1Ni. However, in the 12Cr-1MoVW-2Ni steel, a 5-h temper at 700°C produced a finer subgrain structure with more dislocations and some refinement of the $M_{23}C_6$ precipitation. Again, nickel-doping did not affect the precipitate phases produced in the 12-Cr steels during tempering.

B. HFIR irradiated

HFIR irradiation of 9Cr-1MoVNb and -2Ni at 300 to 500°C produced a dense dislocation structure, considerable coarsening of the subgrain structure, and apparently some dissolution of the as-tempered precipitate structure.

These effects were more pronounced at the lower temperature (see Fig. 3). By contrast, at 600°C, both doped and undoped 9-Cr steels had subgrain and precipitate structures that were similar to or finer than the as-tempered structure (Fig. 3). Most of the smallest as-tempered MC particles appeared to dissolve at 300 to 500°C, while many coarser ones were found after irradiation in both doped and undoped 9Cr steels (see Fig. 7). Irradiation produced additional precipitation in the 9Cr-1MoVNb-2Ni steel at 400 and 500°C but not in the 9Cr-1MoVNb steel. Irradiation of 9Cr-1MoVNb-2Ni at 400°C produced copious amounts of coarse $M_{23}C_6$ [Fig. 2(c)] and fine M_6C (η) particles [Fig. 8(a)], some fine M_2X rods, and a few coarse χ particles (with internal voids). Irradiation at 500°C produced many more coarse χ phase particles with internal voids [Fig. 2(d)], together with abundant, fine M_6C and a few fine M_2X rods.

By contrast, the as-tempered $M_{23}C_6$ carbide and subgrain structures of the doped and undoped 12-Cr steels remained stable during irradiation at various temperatures, with the exception of 12Cr-1MoVW at 500°C. Irradiation produced dislocation loops and/or networks at 300 to 500°C in all steels. But at 500°C, there was considerable coarsening of the subgrain and precipitate structure of the 12Cr-1MoVW during irradiation, as well as replacement of the coarse, as-tempered $M_{23}C_6$ with irradiation-produced M_6C . Fine MC evolved and coarsened during irradiation at 300 to 500°C for all of the 12-Cr steels, and copious amounts of fine M_6C was produced at 400 and 500°C. Similar to the 9-Cr steels, nickel doping caused additional formation of a few coarse χ phase particles (with internal voids) at 400°C, but many more at 500°C. Fine M_2X rods and occasional, fine G-phase particles have thus far been found only in 12Cr 1MoVNb irradiated at 500°C (see Fig. 8).

3.3 Precipitate Compositional Analysis

A. As-tempered

The as-tempered $M_{23}C_6$ phase was mainly rich in Cr, with smaller concentrations of Fe, V, and Mo (see Fig. 9). The composition of the $M_{23}C_6$ did not vary from 9- to 12-Cr steels or change with nickel doping.

The as-tempered MC phase consisted mostly of coarse and fine vanadium-rich MC (VC) particles, with a lesser amount of coarse, mixed V/Nb-rich MC particles [see Fig. 7(a)]. The VC phase was very rich in V (~75 at. %), with smaller amounts of Nb and Cr. The (Nb,V)C had, on average, >50 at. % Nb, a little less V, and small amounts of Cr and Si. The VC carbide was present in all the 9- and 12-Cr steels, but the niobium-rich MC was found only in the 9-Cr steels. Neither phase was affected by nickel doping.

B. HFIR irradiated

The $M_{23}C_6$ phase showed no change in composition during irradiation at 300 to 500°C in any of the steels, except for 9Cr-1MoVNb-2Ni irradiated at 400°C. Samples irradiated at 600°C have not yet been examined. In this case, the copious additional $M_{23}C_6$ produced during irradiation contained less Cr and Mo, and slightly more Fe, Nb, Ni, V, and Si than the as-tempered carbide (see Fig. 9).

Both the V- and Nb-rich MC phases showed compositional changes during HFIR irradiation at 300 to 500°C which were similar in all the 9- and 12-Cr steels, nickel-doped and undoped. The V-rich MC was dominant after irradiation and contained much less V and slightly less Nb while having much more Cr and traces of Si, Ni, Fe, and Mo relative to the as-tempered phase (see Fig. 7). The mixed V/Nb-rich MC phase, which was more abundant after

irradiation, also was much richer in Cr and poorer in V while picking up traces of Mo, Fe, and Si, relative to the as-tempered phase.

During irradiation at 400 and 500°C, the M₆C (η) was the dominant fine precipitate phase produced. Although identification by diffraction analysis is incomplete, the composition of this phase was similar to that found in precipitates in type 316 stainless steel irradiated in HFIR at 425 to 450°C which were positively identified as η phase [20]. The η phase was primarily rich in Cr, Ni, and Si, as shown in Fig. 8, while containing some Fe and traces of Mo, P, and V. The phase composition was identical in nickel-doped 9- and 12-Cr steels, but apparently was enriched only in Si and Cr in the 12Cr-1MoVW steel irradiated at 400°C. Only very coarse η was found in 12Cr-1MoVW steel irradiated at 500°C, but it had the same composition as the fine Cr/Ni/Si-rich η phase shown in Fig. 8.

Traces of fine G-phase were found in 12Cr-1MoVW irradiated at 500°C. This phase was enriched in Si, Ni, and Mn (see Fig. 8). The fine M₂X rods found in 9Cr-1MoVNb-2Ni at 400 and 500°C and 12Cr-1MoVW at 500°C contained mainly Cr and some V, with traces of Mo, Si, and Fe (see Fig. 8).

The large, void-containing χ phase particles observed in the thin foils of the nickel-doped 9- and 12-Cr steels were not found on the extraction replicas for analysis.

4.0 Discussion

Increased void and bubble nucleation in the irradiated nickel-doped steels appears to be a direct consequence of the increased helium generation rather than an artifact caused by the addition of nickel to the alloys. Although nickel doping had no detectable effect on the phase

nature and composition in the as-tempered condition, it does seem to influence the phase evolution in the 9Cr-1MoVNb steel during irradiation at 400 and 500°C. In particular at 400°C in HFIR, the 9Cr-1MoVNb-2Ni steel had abundant irradiation-produced $M_{23}C_6$ and M_6C precipitation whereas the 9Cr-1MoVNb steel did not. However, the comparison of HFIR- and FFTF-irradiated 9Cr-1MoVNb-2Ni steels showed no difference in radiation-produced $M_{23}C_6$ and M_6C precipitation, suggesting that the difference in void evolution clearly correlates with the increased helium generation in HFIR. The fact that nickel-doping does not affect precipitation significantly in the 12-Cr steels with a stable as-tempered structure suggests that the instability of the as-tempered structure in the 9-Cr steel plays some role in subsequent phase evolution during irradiation.

Our data suggest that helium bubble (gas-driven cavities) formation is a crucial, but not sufficient, step in nucleating voids (bias-driven cavities), consistent with a critical-cavity-size theoretical approach to void formation [26]. Further, our data suggest a balance of dislocation and cavity sink strength for matrix void formation only at 400°C. Ideas to explain void resistance of the ferritics based on solute trapping [2] or dislocation loop induced [27,28] reductions in vacancy supersaturation do not seem to explain helium-enhanced void formation. Our data does not appear to answer the questions of intrinsically low steady-state void swelling rates and low biases claimed for the ferritic steels [26,30], because it appears that void nucleation is still occurring. Finally, we see abundant voids together with copious fine precipitation, which seem contrary to the idea that such fine precipitates may contribute to void resistance [11].

Our data are consistent with the idea suggested by Ayrault [30] for ion-irradiated 9Cr-1MoVNb — that subgrain boundaries are strong point-defect sinks in the ferritic steels and that they contribute to void formation resistance when subgrains are small and stable. However, our reactor data at low damage rates and long times indicate far more subgrain instability than he observed during ion irradiation. This may signal the need for caution when looking at ion data to predict void-swelling resistance during neutron irradiation.

Finally, our data indicate that irradiation has strong effects on phase formation and stability coincident with void formation and/or subgrain instability and coarsening. The data further suggest that niobium, silicon, nickel, and especially chromium, are segregating toward precipitates. By contrast, chromium primarily diffuses away from precipitates in irradiated austenitic stainless steels [20]. Our observation of M_6C , χ , and M_2X rods produced during irradiation are consistent with the findings of others [2,31]. However, our observation of M_6C as the primary fine precipitate with only traces of G-phase found at 400 to 500°C differs with Gelles and Thomas [11], who found primarily G-phase and no M_6C . Our observations of irradiation-induced composition modification of $M_{23}C_6$ and MC phases as well as the formation of a silicon/chromium-rich η phase appear to be new findings.

For fusion applications, our results suggest that helium could shorten the incubation period for void formation from projected doses of 150 dpa based on FBR data [14] to perhaps only 50 dpa. With higher helium levels, it is possible that even more voids may form during the incubation period.

The effects of helium on the steady-state void swelling behavior are not known from these experiments, which are still in the low-swelling transient regime, and must be assessed by higher fluence irradiations.

5.0 Conclusions

1. Increased helium (up to 450 appm) enhanced bubble (gas-driven cavity) formation at 300 to 600°C in nickel-doped 9- and 12-Cr steels irradiated in HFIR to ~38 dpa, but voids (bias-driven cavities) formed only at 400 and 500°C.
2. Void formation was maximum at 400°C and greater in 9Cr-1MoVNb-2Ni than the other 9- and 12-Cr steels. However, void swelling was still below 0.5% at ~38 dpa.
3. The absence of bubbles or voids in 9Cr-1MoVNb-2Ni irradiated in FFTF at 407°C to ~47 dpa and ~5 appm He indicates that the void formation of the same steel with a similar microstructure in HFIR at 400°C was due to increased helium generation.
4. As-tempered $M_{23}C_6$ dissolved and the subgrain structures coarsened in the 9-Cr steels irradiated at 300 to 500°C, whereas the microstructure generally remained stable in the 12-Cr steels.
5. Irradiation produced a compositional evolution of the MC phase at 300 to 500°C and produced fine precipitation of primarily M_6C with traces of M_2X and G-phases at 400 and 500°C in the 9- and 12-Cr steels.

References

- [1] S. D. Harkness, B. J. Kestel, and P. Okamoto, Prepared Discussion, p. 334 in: Inter. Conf. Radiation-Induced Voids in Metals, Eds., J. W. Corbett and L. C. Ianniello, CONF-710601 (USAEC, 1972).
- [2] E. A. Little, Rad. Effects 16 (1972) 135.
- [3] K. R. Garr, C. G. Rhodes, and D. Kramer, p. 109 in: Effects of Radiation on Substructure and Mechanical Properties of Metals and Alloys, ASTM-STP-529 (American Society for Testing and Materials, 1973).
- [4] W. G. Johnston et al., J. Nucl. Mater. 54 (1974) 24.
- [5] F. A. Smidt et al., p. 227 in: Irradiation Effects on the Microstructure and Properties of Metals, ASTM-STP-611 (American Society for Testing and Materials, 1976).
- [6] Radiation Effects in Breeder Reactor Structural Materials, Eds., M. L. Bleiberg and J. W. Bennett (The Metallurgical Society of AIME, 1977).
- [7] R. E. Gold et al., Nucl. Technol./Fusion 1 (1981) 169.
- [8] J. I. Bramman et al., *ibid.* ref. 6, p. 479.
- [9] J. J. Huet et al., p. 5 in: Irradiation Behavior of Metallic Materials for Fast Reactor Core Components, Ajaccio, France (CEA, 1979).
- [10] J. Erler et al., *ibid.* ref. 9, p. 11.
- [11] D. S. Gelles and L. E. Thomas, p. 559 in: Proc. Topical Conf. on Ferritic Alloys for Use in Nuclear Energy Technologies, Eds., J. W. Davis and D. J. Michel (The Metallurgical Society of AIME, 1984).
- [12] D. S. Gelles, J. Nucl. Mater. 122 and 123 (1984) 207.
- [13] R. L. Klueh, Nucl. Eng. and Design 72 (1982) 329.
- [14] T. Lechtenberg, J. Nucl. Mater. 133 and 134 (1985) 149.
- [15] R. L. Klueh and M. P. Tanaka, J. Metals 37 (Oct. 1985) 16.
- [16] J. M. Vitek and R. L. Klueh, *ibid.* ref. 11, p. 551.
- [17] J. M. Vitek and R. L. Klueh, J. Nucl. Mater. 122 and 123 (1984) 254.

- [18] D. S. Gelles, p. 129 in: ADIP Semiannu. Prog. Rept., March 31, 1985, DOE/ER-0045/14, Office of Fusion Energy, U.S. Department of Energy.
- [19] P. J. Maziasz, J. Nucl. Mater. 122 and 123 (1984) 472.
- [20] P. J. Maziasz, "Effects of Helium Content on Microstructural Development in Type 316 Stainless Steel under Neutron Irradiation," Oak Ridge National Laboratory report, ORNL-6121 (November 1985).
- [21] L. L. Horton and J. Bentley, *ibid.* ref. 11, p. 569.
- [22] G. Ayrault, p. 182 in: DAFS Quart. Prog. Rept., February 1982, DOE/ER-0046/8, Vol. 1, USDOE, Office of Fusion Energy.
- [23] R. L. Klueh, J. M. Vitek, and M. L. Grossbeck, p. 648 in: Effects of Irradiation on Materials: Eleventh Conf., ASTM-STP-782, Eds., H. R. Brager and J. S. Perrin (American Society for Testing and Materials, 1982).
- [24] M. L. Grossbeck, J. W. Woods, and G. A. Potter, p. 36 in: ADIP Quart. Prog. Rept., Sept. 30, 1980, DOE-ER-0045/4, Office of Fusion Energy, U.S. Department of Energy.
- [25] L. R. Greenwood, p. 22 in: ADIP Semiannu. Prog. Rept., March 31, 1985, DOE/ER-0045/14, Office of Fusion Energy, U.S. Department of Energy.
- [26] L. L. Horton and L. K. Mansur, p. 344 in: Effects of Radiation on Materials: Twelfth International Symposium, ASTM-STP-870, eds., F. A. Garner and J. S. Perrin (American Society for Testing and Materials, 1985).
- [27] E. A. Little, R. Bullough, and H. M. Wood, Proc. Royal Soc. A372 (1980) 565.
- [28] R. Bullough, H. M. Wood, and E. A. Little, p. 593 in: Effects of Irradiation on Materials: Proc. Tenth International Symposium, ASTM-STP-725, eds., D. Kramer, H. R. Brager, and J. S. Perrin (American Society for Testing and Materials, 1981).
- [29] J. J. Sniegowski and W. G. Wolfer, *ibid.*, ref. 11, p. 579.
- [30] G. Ayrault, J. Nucl. Mater. 114 (1983) 34.
- [31] L. P. Stoter and E. A. Little, p. 369 in: Conf. Proc. Advances in Physical Metallurgy and Applications of Steels (The Metals Society-London, 1981).

Table 1. Compositions of 9Cr-1MoVNb and 12Cr-1MoVW heats of steel with and without nickel doping

Alloy designation	Heat number	Concentration ^a (wt %)										
		Cr	Mo	Ni	Mn	C	Si	V	Nb	Ti	W	N
9Cr-1MoVNb	(XA 3590)	8.6	1.0	0.1	0.36	0.09	0.08	0.21	0.063	0.002	0.01	0.05
9Cr-1MoVNb-2Ni	(XA 3591)	8.6	1.0	2.2	0.36	0.064	0.08	0.22	0.066	0.002	0.01	0.05
12Cr-1MoVW	(XAA 3587)	12.0	0.9	0.4	0.5	0.2	0.18	0.27	0.018	0.003	0.54	0.02
12Cr-1MoVW-1Ni	(XAA 3588)	12.0	1.0	1.1	0.5	0.2	0.13	0.31	0.015	0.003	0.53	0.02
12Cr-1MoVW-2Ni	(XAA 3589)	11.7	1.0	2.3	0.5	0.2	0.14	0.31	0.015	0.003	0.54	0.02

^aBalance iron.

Table 2. Normalizing and tempering conditions for various steels

Alloy designation	Normalization	Tempering
9Cr-1MoVNb	0.5 h @ 1040°C	1 h @ 760°C
9Cr-1MoVNb-2Ni	0.5 h @ 1040°C	5 h @ 700°C
12Cr-1MoVW	0.5 h @ 1050°C	2.5 h @ 780°C
12Cr-1MoVW-1Ni	0.5 h @ 1050°C	2.5 h @ 780°C
12Cr-1MoVW-2Ni	0.5 h @ 1050°C	5 h @ 700°C

LIST OF FIGURES

Fig. 1. Helium generation plotted versus displacement damage level for undoped and 2 wt % Ni-doped 9Cr-1MoVNb irradiated in FFTF, HFIR, and a fusion first wall.

Fig. 2. Microstructures of (a),(b) 9Cr-1MoVNb (~32 appm He) and (c),(d) 9Cr-1MoVNb-2Ni (410 appm He) irradiated in HFIR at 400 and 500°C to ~37 to 39 dpa. High magnification insets show bubbles in (c) and (d), *but almost none in (a)*

Fig. 3. Microstructural comparison of the subgrain structure of 9Cr-1MoVNb-2Ni (a) as-tempered and after HFIR irradiation to ~37 to 39 appm and 410 appm He at (b) 300°C, and (c) 600°C. High magnification insets show bubbles in (b) and (c).

Fig. 4. Microstructures of 9Cr-1MoVNb-2Ni irradiated in (a) FFTF at 407°C to 47 dpa and 5 appm He and (b) HFIR at 400°C to ~37 dpa and 410 appm He. Precipitate and dislocation microstructures about the same for both samples, but void formation increases with helium content.

Fig. 5. Microstructures of (a) 12Cr-1MoVW (87 appm He), (b) 12Cr-1MoVW-1Ni (217 appm He), and (c) 12Cr-1MoVW-2Ni (440 appm He) irradiated in HFIR at 407°C to 36 to 39 dpa.

Fig. 6. Microstructures of the subgrain structure of 12Cr-1MoVW (a) as-tempered and after HFIR irradiation at (b) 300°C, and (c) 500°C to 37 to 39 dpa and ~87 appm He.

Fig. 7. Micrographs of precipitate extraction replicas of 9Cr-1MoVNb (a) as-tempered and (b) HFIR irradiated at 400°C to 37 dpa and 32 appm He. Compositional histograms of MC phase particles determined by quantitative XEDS analysis are included for each specimen. Note the particle coarsening and compositional evolution for (b) compared to (a).

Fig. 8. Micrographs of precipitate extraction replicas from (a) 9Cr-1MoVNb-2Ni irradiated in HFIR at 400°C to 37 dpa and 410 appm He, and (b) 12Cr-1MoVW irradiated in HFIR at 500°C to 38 dpa and 87 appm He. Histograms show phase compositions determined from quantitative XEDS for fine (c) M_6C (η) particles from (a), and (d) G-phase, and (e) M_2X rods from (b).

Fig. 9. Comparison of phase compositions for particles analyzed via quantitative XEDS on extraction replicas from 9Cr-1MoVNb-2Ni (a) as-tempered and (b) after irradiation at 400°C to 37 dpa and 400 appm He.

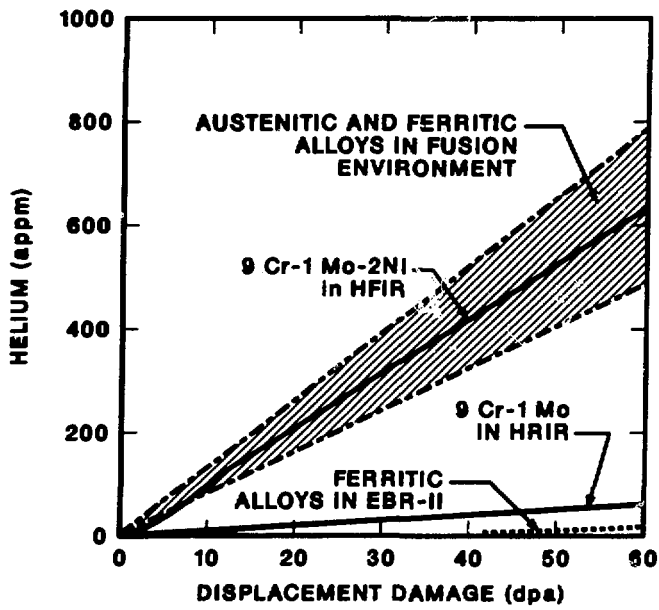


Fig. 1.

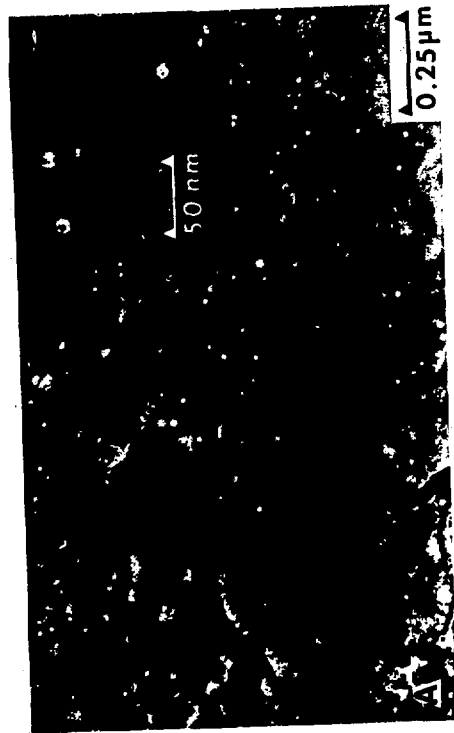


Fig. 2.

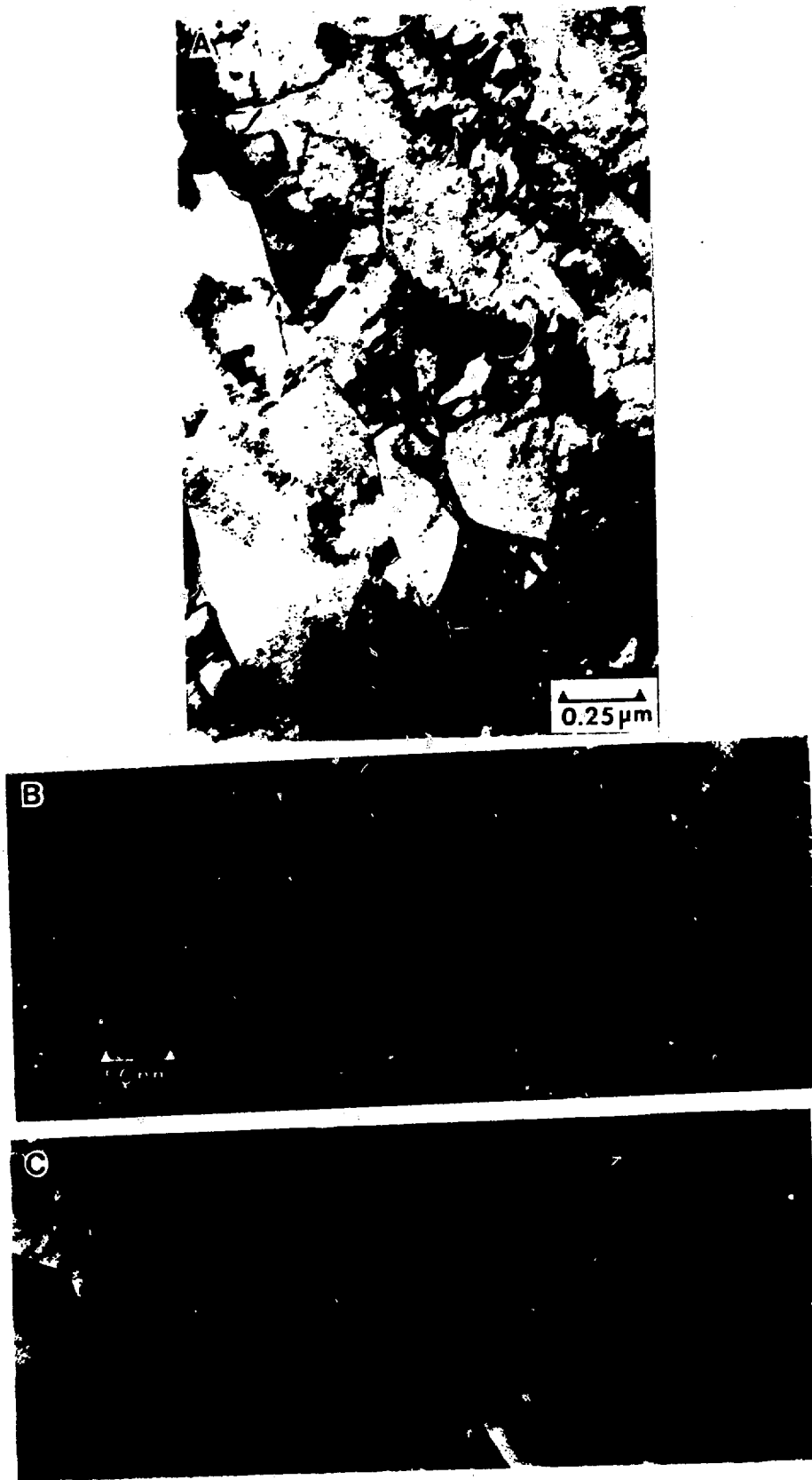


Fig. 3.

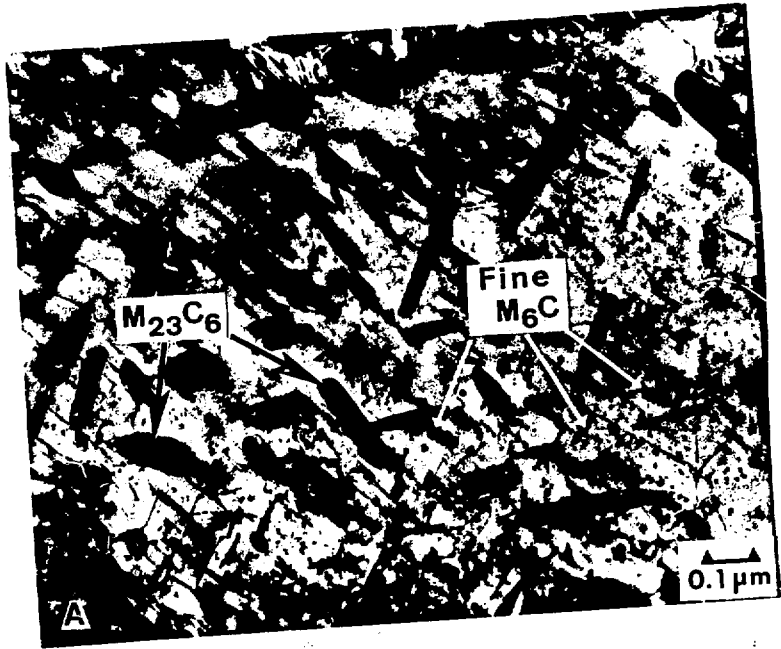


Fig. 4.



Fig. 5.

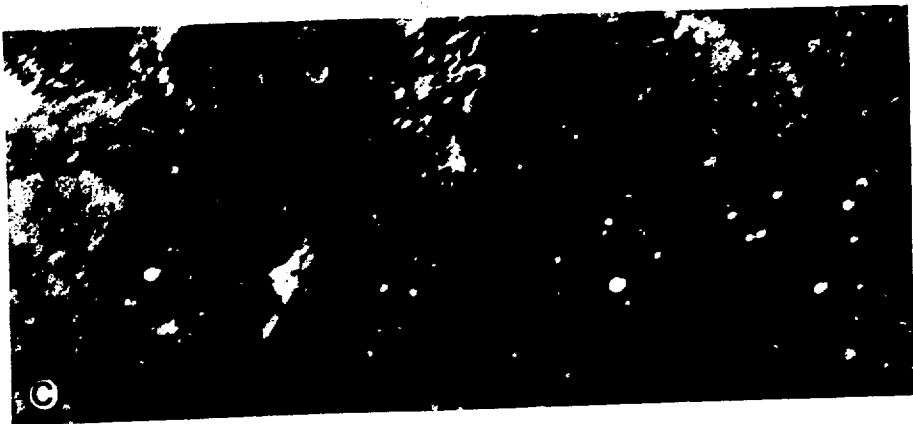
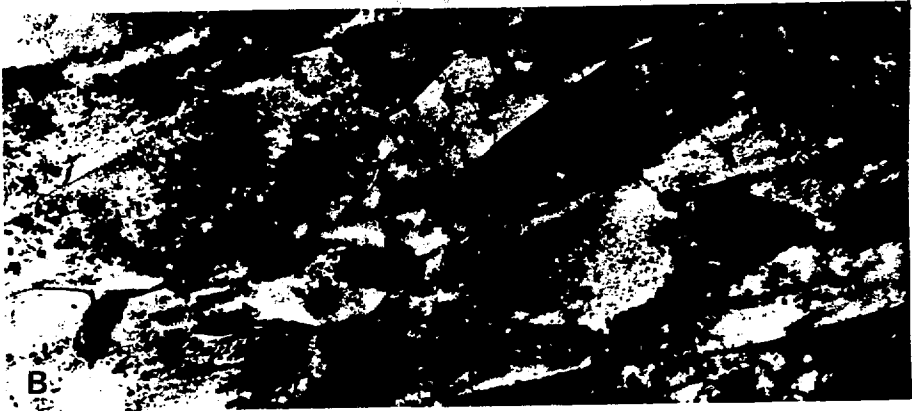


Fig. 6.

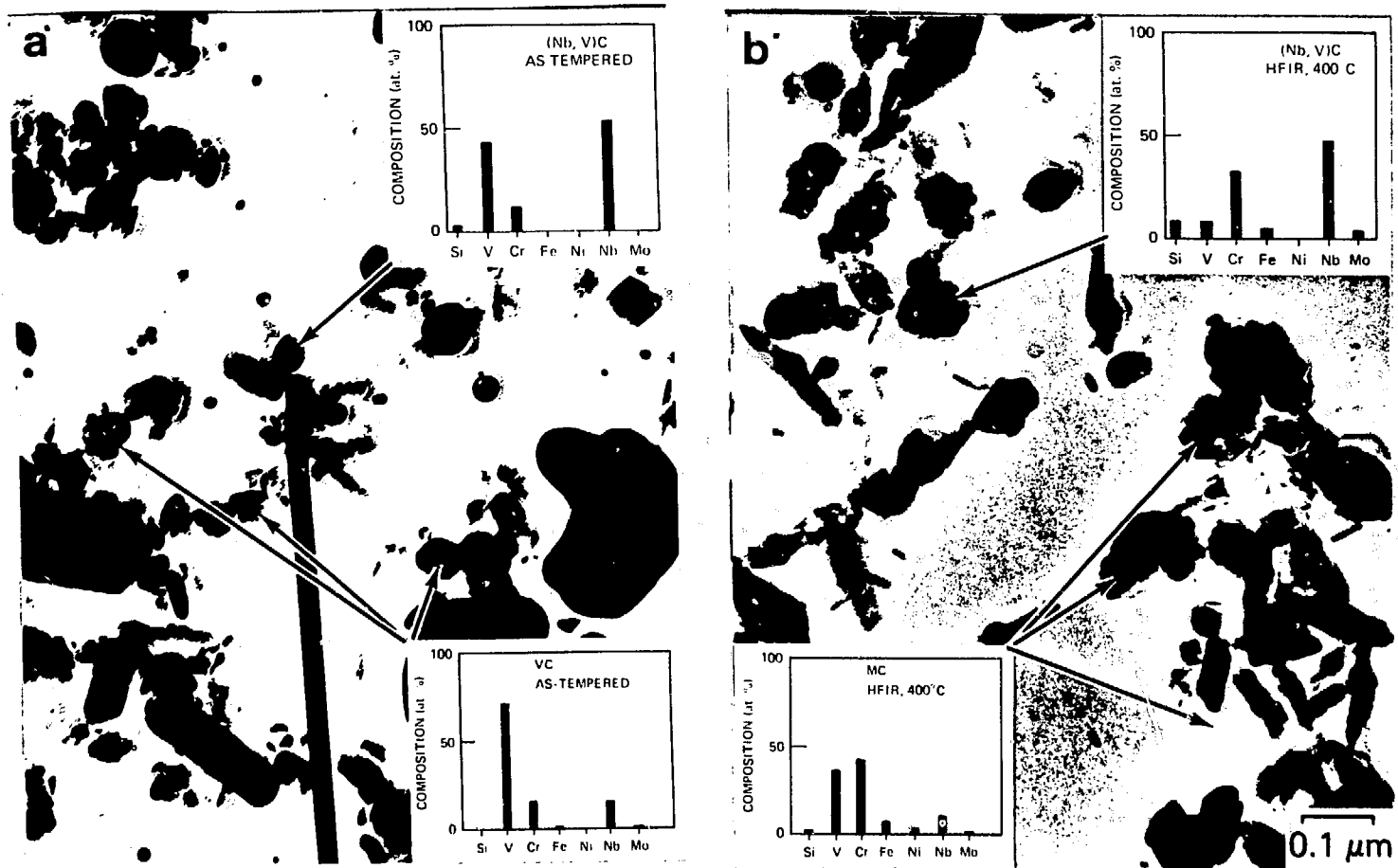


Fig. 7.

EXTRACTION REPLICAS

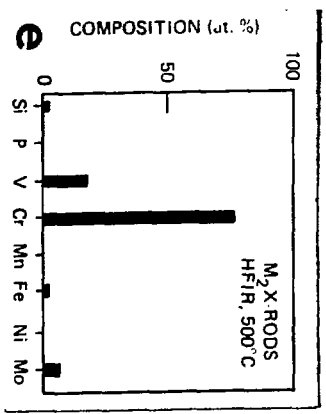
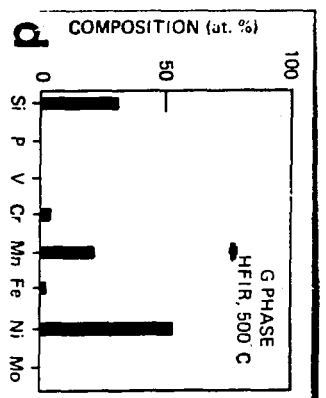
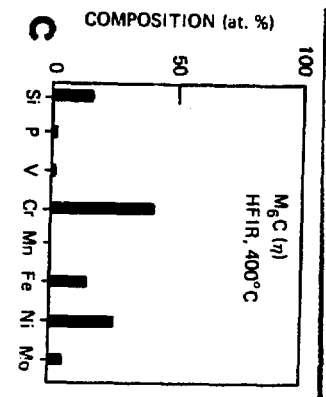


Fig. 8.

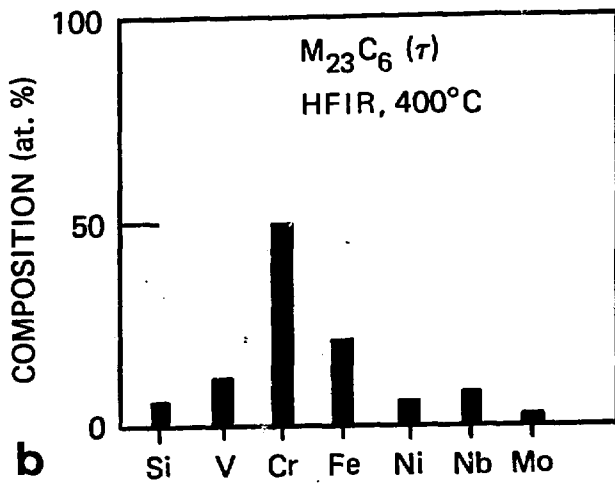
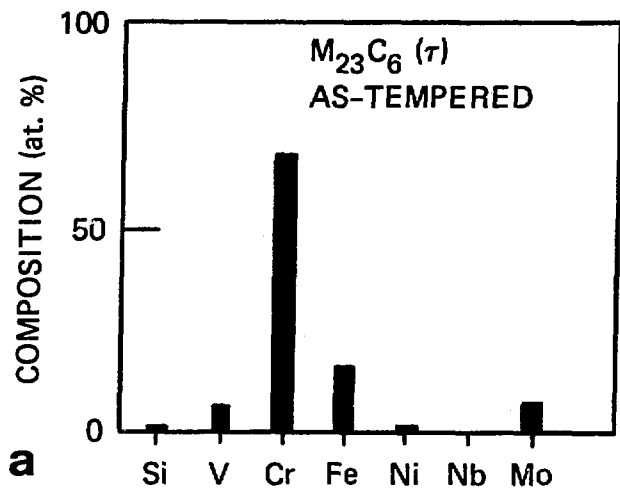


Fig. 9.